FEBS Letters 584 (2010) 1536–1542

FEBS Letters

journal homepage: www.FEBSLetters.org

Solution structure and dynamics of mouse ARMET

Jun Hoseki [a], Hiroaki Sasakawa [b,c], Yoshiki Yamaguchi [b,1], Momoe Maeda [a], Hiroshi Kubota [a,2], Koichi Kato [b,c,d], Kazuhiro Nagata [a,*]

[a] Department of Molecular and Cellular Biology, Institute for Frontier Medical Sciences, Kyoto University, 53 Kawahara-cho, Shogoin, Sakyo-ku, Kyoto 606-8507, Japan
[b] Graduate School of Pharmaceutical Sciences, Nagoya City University, Tanabe-dori 3-1, Mizuho-ku, Nagoya 467-8603, Japan
[c] Institute for Molecular Science, National Institutes of Natural Sciences, 5-1 Higashiyama, Myodaiji, Okazaki 444-8787, Japan
[d] Okazaki Institute for Integrative Bioscience, National Institutes of Natural Sciences, 5-1 Higashiyama, Myodaiji, Okazaki 444-8787, Japan

ARTICLE INFO

Article history:
Received 16 February 2010
Revised 16 February 2010
Accepted 2 March 2010
Available online 6 March 2010

Edited by Judit Ovádi

Keywords:
ER stress
Solution structure
Positive charge
Domain movement

ABSTRACT

ARMET is an endoplasmic reticulum (ER) stress-inducible protein that is required for maintaining cell viability under ER stress conditions. However, the exact molecular mechanisms by which ARMET protects cells are unknown. Here, we have analyzed the solution structure of ARMET. ARMET has an entirely α-helical structure, which is composed of two distinct domains. Positive charges are dispersed on the surfaces of both domains and across a linker structure. Trypsin digestion and ^{15}N relaxation experiments indicate that the tumbling of the N-terminal and C-terminal domains is effectively independent. These results suggest that ARMET may hold a negatively charged molecule using the two positively charged domains.

1. Introduction

Cells are continuously exposed to various stresses caused by environmental changes. These stresses often lead to the accumulation of unfolded or misfolded proteins, which are toxic to cells. Thus, various cellular defense mechanisms are adapted to cope with the toxicity of the aberrant proteins.

The endoplasmic reticulum (ER) is a major site of protein synthesis. ER quality control (ERQC) mechanisms monitor protein folding and the transport of immature proteins is prevented. Misfolded/unassembled proteins are discarded by a process called ER-associated degradation (ERAD) [1]. When ER stresses, such as oxidative stress, genetic mutation or viral infection, overwhelm the capacity of the ERQC system, unfolded or misfolded proteins accumulate in the ER. The accumulation of these aberrant proteins is sensed through three ER stress sensor proteins, PERK, IRE1 and ATF6, resulting in the activation of an intracellular signal transduction pathway called the unfolded protein response (UPR) [2]. The UPR increases the expression of several target genes to restore ER homeostasis. UPR target genes possess a broad array of functions including protein folding, protein glycosylation, ERAD, oxidative stress response, secretory protein trafficking, and lipid biosynthesis [3].

The Akita mouse is a diabetes model and has a C96Y mutation in the *Ins2* gene, which causes insulin misfolding and aggregation by formation of improper disulfide bonds [4,5]. This proinsulin mutant is prone to aggregation due to the exposure of hydrophobic surfaces of the protein [6]. We previously identified the Arginine rich, mutated in early stage of tumors (ARMET) gene as a gene upregulated in pancreatic β cells expressing the C96Y mutant. ARMET encodes a soluble ER-resident protein with a KDEL-like ER retention signal at the C-terminus and is upregulated by ER stress via the ER stress response element-II [7]. RNAi-mediated knockdown of ARMET expression induced the UPR in HeLa cells and stable overexpression of ARMET was shown to protect cells from the toxic effect by the treatment with ER stress inducers [8]. These findings suggest that ARMET is an essential gene for cell survival under ER stress conditions.

Abbreviations: ARMET, Arginine rich, mutated in early stage of tumors; DSS, 2,2-dimethyl-2-silapentane-5-sulfonic acid; bHLH, basic-helix–loop–helix; ER, endoplasmic reticulum; ERAD, ER-associated degradation; ERQC, ER quality control; HSQC, heteronuclear single quantum coherence; NOE, nuclear Overhauser effect; NOESY, nuclear Overhauser enhancement spectroscopy; RMSD, root-mean-square deviation; TOCSY, total correlated spectroscopy; UPR, unfolded protein response

* Corresponding author. Fax: +81 75 751 4645.
E-mail address: nagata@frontier.kyoto-u.ac.jp (K. Nagata).
[1] Present address: Structural Glycobiology Team, Systems Glycobiology Research Group, Chemical Biology Department, RIKEN, Advanced Science Institute, 2-1 Hirosawa Wako, Saitama 351-0198, Japan.
[2] Present address: Department of Life Science, Faculty of Engineering and Resource Science, Akita University, Akita 010-8502, Japan.

0014-5793/$36.00 © 2010 Federation of European Biochemical Societies. Published by Elsevier B.V. All rights reserved.
doi:10.1016/j.febslet.2010.03.008

ARMET is also called mesencephalic astrocyte-derived neurotrophic factor (MANF) and was identified as a neurotrophic factor specific for dopaminergic neurons in conditioned medium of ventral mesencephalic cell line 1 [9]: ARMET had protective activity for dopaminergic neurons but not that of GABAergic or serotonergic neurons. Although the previous study indicated that ARMET transfected into the cells was secreted, the additional tags added after ER retention signal at the C-terminus of ARMET used in such studies might prevent its retention in the ER [8–10]. Actually, only small amount of endogenous ARMET was shown to be secreted [8]. On the other hand, in *Drosophila,* dopaminergic neuritis was markedly decreased in ARMET knockout embryo, while larvae were lethal after the knockout of ARMET [10]. Thus, secreted ARMET may play a vital role as a neurotrophic factor for maintenance of dopaminergic neurons.

These observations indicate that ARMET is required for cell protection against ER stress and critical for specific neuronal cells to survive. However, the exact molecular mechanisms by which ARMET exert the cell protective functions are still unknown. Here, we report the NMR structure and dynamics of mouse ARMET and discuss the possible role of the ARMET structure in binding other molecules. This is the first report of a solution structure of an ARMET family protein.

2. Materials and methods

2.1. Expression and purification of the ARMET protein

For the production of ^{15}N-labeled proteins, *Escherichia coli* strain Origami B (DE3) cells carrying a 6xHis-tagged ARMET expression plasmid [7] were grown in M9 minimal medium using $^{15}NH_4Cl$ (1 g/L) as the sole nitrogen source. In addition to the nitrogen source, ^{13}C-glucose (2 g/L) was used as the sole carbon source for the production of ^{15}N/^{13}C-labeled proteins. After the bacteria were grown up to an OD_{600} = 1.0, IPTG (0.5 mM) was added to the culture. The bacteria were cultured for an additional four hours at 37 °C and harvested by centrifugation at 6680×*g* for 15 min. The cells were lysed by sonication, centrifuged at 26 740×*g* for 30 min, and the supernatant collected. His-tagged protein was purified from the supernatant by Ni^{2+} affinity chromatography, and NMR samples were prepared at a concentration of 1 mM in 90% H_2O/10% D_2O (v/v), 10 mM sodium phosphate buffer at pH 6.0. For trypsin digestion, untagged mature mouse ARMET was prepared as follows. The ARMET cDNA was amplified and subcloned into the *NdeI* and *BamHI* sites of pET21a (Novagen). The expression and purification of the untagged mature ARMET were performed as described previously [7].

2.2. Mass spectrometry analyses for determination of disulfide bond arrangements

Purified untagged recombinant ARMET was cleaved by lysyl endopeptidase in solution. Alternatively, ARMET was separated by SDS–PAGE using 15% gel under non-reducing condition, blotted onto a polyvinylidene fluoride membrane, digested by lysyl endopeptidase and subsequently digested by V8 protease. Matrix-assisted laser desorption/ionization time of flight (MALDI-TOF) mass spectrometry of the digested products was carried out to detect peptides containing disulfide bonds. MALDI-TOF MS spectra were measured with Voyager-DE STR (Applied Biosystems).

2.3. NMR spectroscopy and structural determination

NMR spectral measurements were performed using a JEOL ECA920 spectrometer employing the GORIN application [11], as well as Bruker Avance 600 and DMX500 spectrometers equipped with 5-mm inverse triple-resonance probes with three-axis gradient coils. Backbone and Cβ resonances were assigned sequentially using 2D ^{1}H–^{15}N heteronuclear single quantum coherence (HSQC), ct-^{1}H–^{13}C HSQC, and 3D HNCA experiments, as well as HN(CO)CA, HNCO, HN(CA)CO, CBCA(CO)NH and NHCACB spectra. Backbone assignments were confirmed by 3D ^{13}C-edited nuclear Overhauser enhancement spectroscopy (NOESY) and ^{15}N-edited NOESY spectra. Side chain and Hα assignments were obtained from 3D HBHA(-CO)NH, ^{15}N-edited total correlated spectroscopy (TOCSY), H(CCO)NH, C(CO)NH, HCCH-COSY and HCCH-TOCSY spectra. Aromatic proton assignments were conducted using 2D ^{1}H–^{1}H TOCSY and ^{1}H–^{1}H NOESY spectra. The time domain data were processed with the nmrPipe software package [12] and semiautomatic resonance assignment was carried out using the Olivia software (http://fermi.pharm.hokudai.ac.jp/olivia/).

The ^{1}H chemical shifts were referenced to external 2,2-dimethyl-2-silapentane-5-sulfonic acid (DSS). The ^{13}C and ^{15}N chemical shifts were indirectly referenced to DSS using the absolute frequency ratios.

Distance restraints were constructed from intensities of NOE cross peaks in 2D NOESY, 3D ^{15}N-edited NOESY and ^{13}C-edited NOESY spectra with a 100 ms mixing time. A macro CALIBA in the CYANA software [13] was used for the calibration of distance restraints. NOE cross peaks were initially assigned based on the chemical shift data and the NOE assignments were iteratively checked and corrected during the structure calculations. Backbone dihedral angle restrains were derived from chemical shift data using TALOS software [14]. The structural determination of ARMET was conducted using the CYANA software [15]. In the calculations, distance limits were used to enforce disulfide bonds (Cys19–Cys106, Cys53–Cys64, Cys22–Cys95 and Cys140–Cys143) which were determined by the MS analyses (see the Section 3). The atomic coordinate data have been deposited in the Protein Data Bank (accession code 2RQY).

^{15}N longitudinal spin-relaxation times (T_1) were measured with relaxation delays of 20, 50, 80, 120, 200, 400, 600, 900, 1200 and 1600 ms. ^{15}N transverse relaxation times (T_2) were obtained with ^{15}N 180° CPMG pulses at total relaxation delays of 16, 32, 48, 64, 80, 96, 128, 160 and 192 ms. For T_2 measurements, temperature-compensating ^{15}N 180° pulses were applied during the recycle delay. ^{15}N{^{1}H} nuclear Overhauser effects (NOE) were obtained by interleaving pulse sequences with and without proton saturation.

2.4. Trypsin digestion

Untagged purified ARMET protein (0.18 mg/ml) was digested with 0.01 mg/ml TPCK-treated trypsin (Sigma) at 30 °C in 50 mM sodium phosphate buffer (pH 8.0). The reaction was stopped by adding Laemmli SDS sample buffer containing dithiothreitol and boiling for 5 min. The digested products were separated by SDS–PAGE in a NuPAGE® 10% Bis-Tris gel (Invitrogen) with MES running buffer under reducing conditions, and blotted on a polyvinylidene difluoride membrane. Bands stained with Coomassie brilliant blue were excised from the membrane and N-terminal amino acid sequences of the digested products were determined using a protein sequencer.

3. Results and discussion

3.1. Solution structure of ARMET

The ^{1}H–^{15}N HSQC spectrum of ^{15}N-labeled ARMET possessed well-dispersed signals (Fig. 1). With the combined information from all heteronuclear experiments, the backbone amide protons

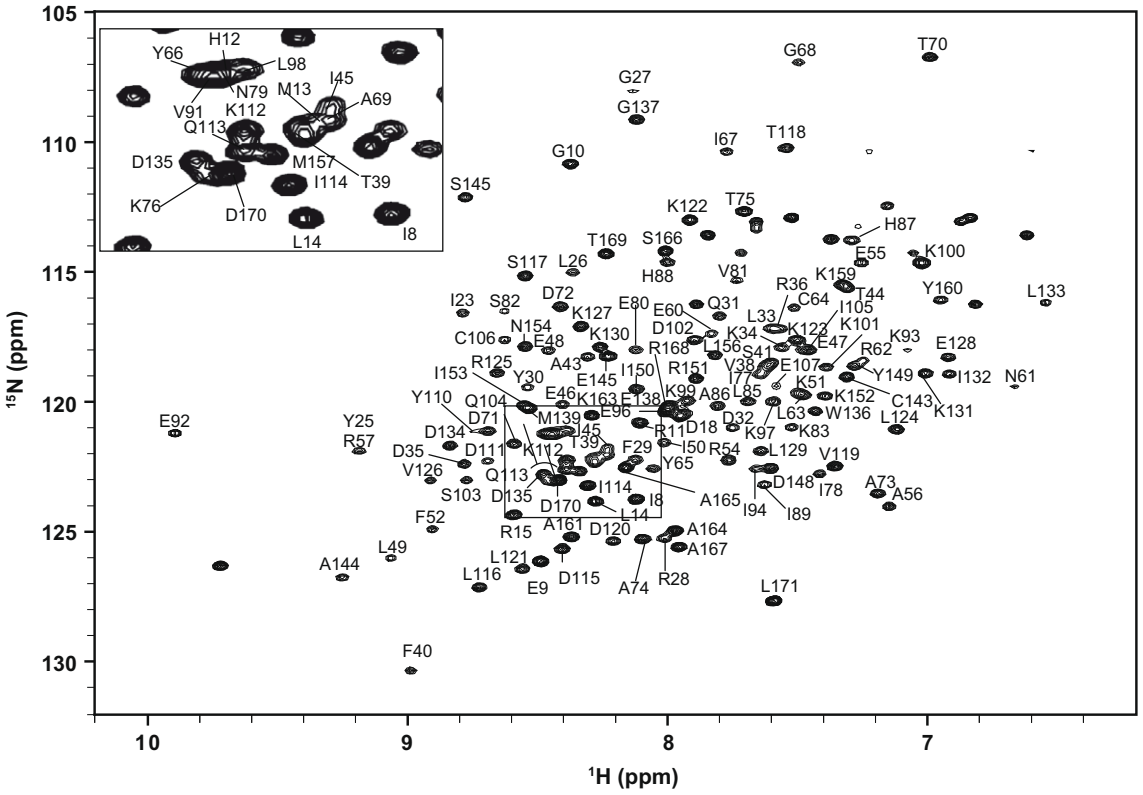

Fig. 1. ^{1}H–^{15}N HSQC spectrum of ^{15}N-labeled ARMET. The spectrum was recorded at 310 K on a BrukerDMX500 spectrometer equipped with a cryogenic probe. Backbone amide cross peaks are indicated with amino acid assignments.

and ^{15}N nuclei of ARMET were assigned, with the exception of the proline residues. Residues 107–111 have weak signal intensity in the HSQC spectrum because of signal broadening, suggesting that these residues fluctuate on a millisecond-scale.

ARMET homologs have eight conserved cysteines. As ARMET has no free sulfhydryl groups and was eluted in a monomer fraction by gel filtration chromatography, ARMET appears to have four intramolecular disulfide bonds [7]. To determine the cysteine pairs in ARMET in advance of the determination of ARMET solution structure, MALDI-TOF MS analyses were performed after digestion of ARMET by lysyl endopeptidase or sequential digestion by lysyl endopeptidase and V8 protease. Peptides containing disulfide bond (Cys53–Cys64 or Cys140–Cys143) were detected with the strongest signals by both analyses (Table S1). The MS analysis of lysyl endopeptidase-digested ARMET showed that the peptide containing Cys19 and Cys22 (AA 13–34) was linked with either or both of the peptide containing Cys95 (AA 94–97) and the peptide containing Cys106 (AA 102–109) via disulfide bonds. Peptide containing disulfide bond Cys19–Cys106 was detected by the analysis of the double digested ARMET. Thus, ARMET mainly forms the following four disulfide bonds: Cys19–Cys106, Cys53–Cys64, Cys22–Cys95 and Cys140–Cys143. Although disulfide bond between Cys95 and Cys143 was detected only by the MS analysis of the double digested ARMET, it may be a minor arrangement in recombinant ARMET protein.

The solution structures of ARMET were calculated using the disulfide bond constraints determined by the MS analyses. The statistics of the ARMET solution structures are summarized in Table 1. ARMET is composed of two distinct domains (Fig. 2), despite a relatively small molecular weight (18 kDa). A flexible region, where signal broadening was observed in the HSQC spectrum (Fig. 1), links the two domains. Consistent with the previous finding that ARMET has two conserved CXXC motifs (19CXXC22 and 140CXXC143) containing no redox-active cysteines [7], the overall structure of ARMET is not a thioredoxin fold (an α/β structure) but an entirely α-helical structure (Fig. 2). The N-terminal domain (N-domain, 18-108) is comprised of six helices (Fig. 2A). Excluding α3 and 3/10 helices, the four helices (α1, α2, α4, π) constitute a four-

Table 1
ARMET structural statistics.

(A) Restraints used in the structure calculations		
Total number of distance restraints	1514	
Intra-residue ([$i = j$])	364	
Sequential ([$\|i - j\| = 1$])	442	
Medium range ([$1 < \|i - j\| < 5$])	516	
Long range ([$\|i - j\| \geqq 5$])	188	
Number of torsion angle restraints $\varphi\psi$	58/59	
(B) Geometric statistics		
RMSD from the mean structure[a] (Å)		
Backbone atoms (residues 24–69 and 78–95)	0.491 (N-domain)	
(residues 123–138 and 144–158)	0.599 (C-domain)	
Heavy atoms (residues 24–69 and 78–95)	1.03 (N-domain)	
(residues 123–138 and 144–158)	1.07 (C-domain)	
(C) Structure quality factors		
	Mean score	*Z*-score
Procheck *G*-factor (φ/ψ)	−0.62	−2.12
Procheck *G*-factor (all dihedral angle)	−0.95	−5.62
Verify 3D	0.20	−4.17
Prosall (−ve)	0.35	−1.24
MolProbity clashscore	25.63	−2.87
(D) Ramachandran analysis (%)		
Most favored regions	81.0	
Additional allowed regions	17.5	
Generously allowed regions	1.5	
Disallowed regions	0.0	

[a] Mean coordinates were obtained by averaging the coordinates of 10 calculated structures.

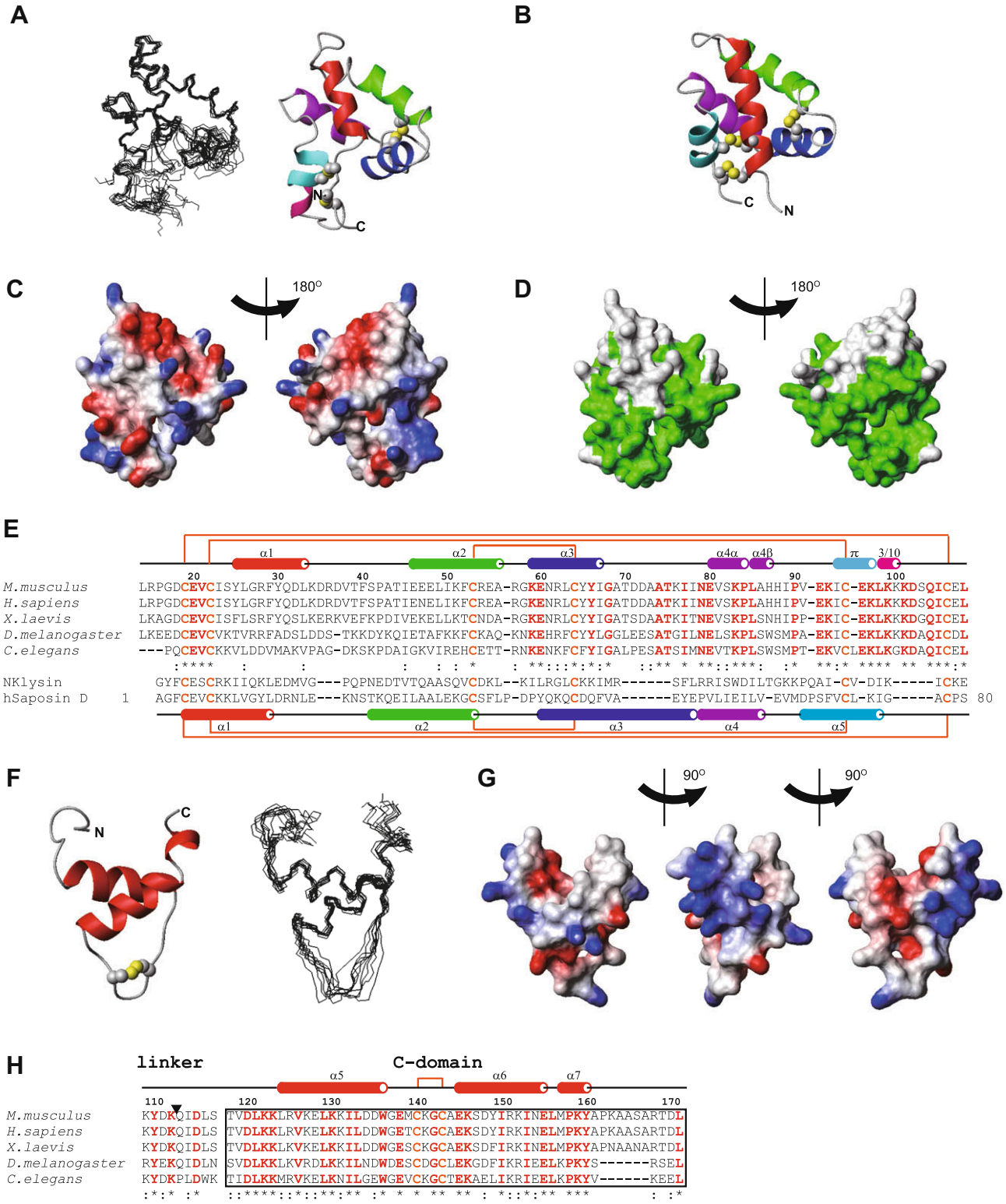

Fig. 2. Solution structure of ARMET. (A) Superimposition of 10 energy-minimized conformers (left) and a ribbon representation (right) of the N-domain. The best fitting structures of the conformers are super-imposed (RMSD of backbone atoms = 0.49 Å). The averaged coordinates were used to draw the ribbon structure. (B) Structure of human saposin D was aligned to the mean structure of the N-domain shown in Fig. 2A. (C) Electrostatic surfaces of the N-domain were calculated and drawn using the MOLMOL program [22]. The negative and positive charges are shown in red and blue, respectively. The orientation of the model on the left in (C) corresponds to that in Fig. 2A. (D) Conserved amino acids on the surface of the N-domain are indicated in green. (E) Sequence alignments of the N-domain of the ARMET family proteins and saposin D. The sequences of the ARMET family proteins were aligned using CLUSTAL W. The alignment of ARMET proteins and saposin D is based on structural homology. (F) Superposition of a ribbon representation (left) and 10 conformers (right) of the C-domain. (G) Electrostatic surface of the C-domain. (H) Sequence alignments of the C-domain of the ARMET family proteins. All the graphics were drawn using the MOLMOL software.

helix bundle-like structure. The N-domain contains a π-helix (93-97), which is a rare secondary structure. Most π-helices are involved in binding enzyme substrates or ligand molecules [16]. Three disulfide bonds are found in the N-domain: Cys19–Cys106

and Cys22–Cys95 connect a loop at the N-terminus to a loop structure at the end of the N-domain and the π-helix, and Cys53–Cys64, connects the α2 helix, which is included in the helix bundle-like structure, to the α3 helix. The disulfide bond between Cys53 and Cys64 stabilize the N-domain structure whereas the region containing the two other disulfide bonds are still flexible (Figs. 2A and S1). Observation of large root-mean-square deviation (RMSD) of backbone atoms of the loop between the α3 and α4 helices indicates that this loop is flexible (Figs. 2A and S1). The electrostatic charges of the ARMET N-domain are dispersed over the entire surface (Fig. 2C). The positively charged residues, which are located on the π-helix and the 3/10 helix, are conserved among ARMET homologs, but the negatively charged residues on the α2 helix are not (Fig. 2C and D). These data suggest that the positively charged area

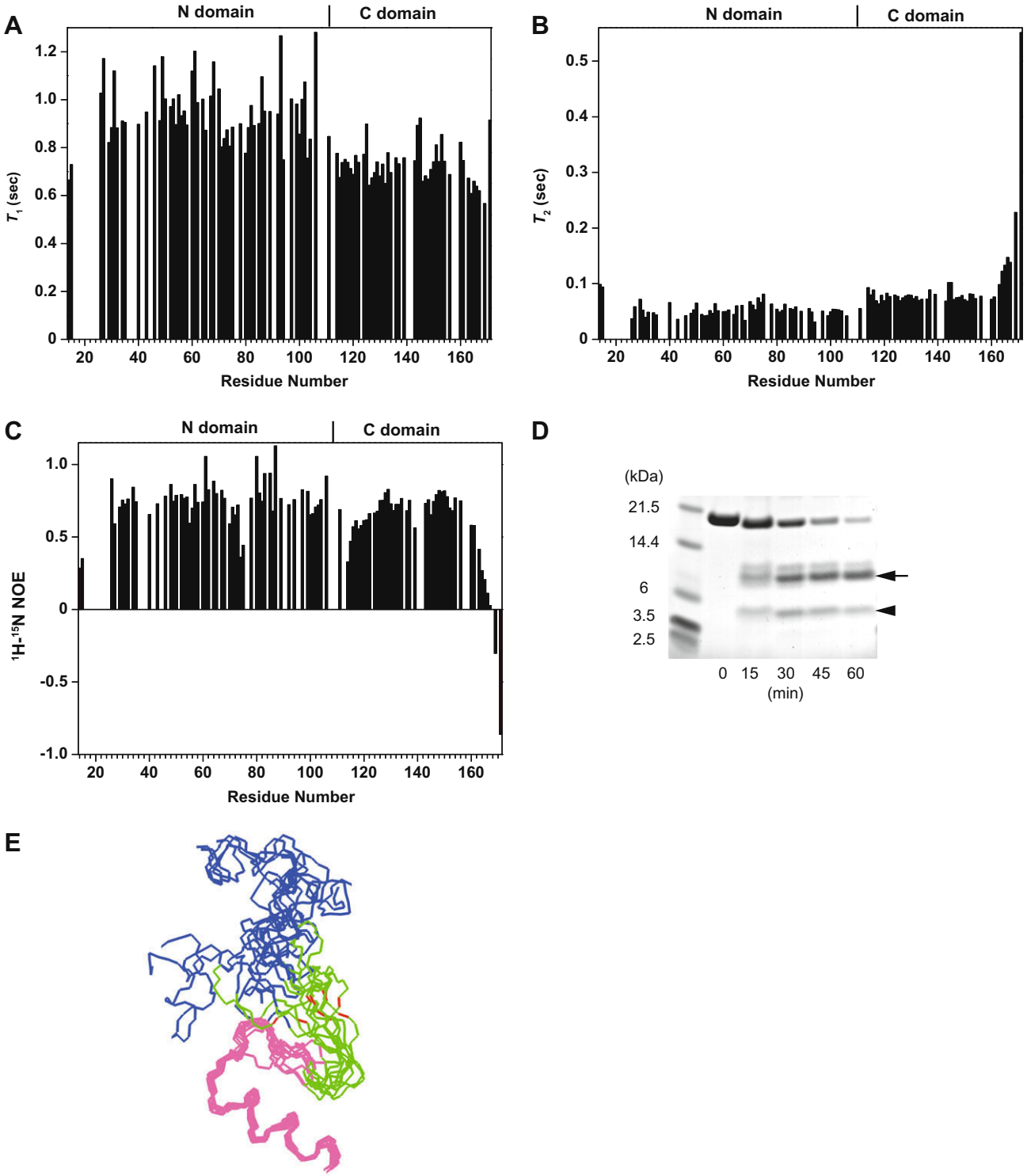

Fig. 3. Solution dynamics of the two domains in ARMET. ^{15}N spin-lattice relaxation time (T_1) (A), spin–spin relaxation time (T_2) (B), and ^{1}H-^{15}N nuclear Overhauser effects (NOE) (C) of backbone N atoms. (D) Trypsin digestion of ARMET. Aliquots of digested ARMET were removed at indicated times and separated by SDS–PAGE. The N-terminal amino acid sequences of the digested fragments were determined using a protein sequencer. (E) Superposition of 10 conformers containing regions near the linker structure of ARMET. The structures of residues 93-136 are super-imposed for best fit of the helices of the C-domain (123–136, in pink). The C-terminal part of the N-domain, the linker, and trypsin digested bonds in ARMET are drawn in blue, green and red, respectively.

containing the π-helix might be important in the cellular function of ARMET.

The Dali server indicated that the crystal structures of the N-domain of ARMET and of ARMET-like protein 1 (ARMET-L1) [17,18], correspond well to the N-domain of our solution structure. ARMET-L1 shows a high homology (about 60%) to ARMET and was shown to have neuroprotective activity for dopaminergic neurons [8]. While ARMET was induced by ER stress [7], ARMET-L1 was not [8]. The Dali server also found several saposin-like fold proteins (saposins, NK-lysin, granulysin, amoebapore) with a weak but significant similarity ($Z > 3.0$) to the N-domain. Saposin-like proteins have remarkable sequence variability and exert their cellular functions by interacting with various molecules [19]. Saposin D (PDB code: 2RB3) exhibits the closest alignment with the N-domain of ARMET ($Z = 4.6$, RMSD between backbone atoms = 2.8 Å) (Fig. 2B). The topology of secondary structure elements of the N-domain is similar to that of saposin D and arrangement of disulfide bonds in both structures is identical (Figs. 2A, B and E, and S2). Saposins are required for the degradation of plasma membrane derived glycosphingolipids in the lysosome [20]. They interact with the glycolipids and promote their degradation by recruiting them to hydrolases. Saposins have a hydrophobic patch, which is assumed to be a lipid binding site, on the surface [21]. In contrast, the charged surface of the ARMET N-domain (Fig. 2C) suggests that interacting molecules may differ considerably between ARMET and saposins.

The solution structure of the C-terminal domain (C-domain) was determined clearly in the present study (Fig. 2F), although the C-domain of the crystal structure previously reported was disordered [17]. The C-domain is well conserved among the ARMET family proteins, while the backbone structure of the C-domain is more flexible than that of the N-domain (Figs. 2A, F, H, and S2 and Table 1). A disulfide bond between conserved cysteines (Cys140 and Cys143) in the CXXC motif of the C-domain is found in a loop structure between the α5 and the α6 helix, suggesting that it restricts the flexibility of the loop. The C-domain structure (118–162) is composed of a basic-helix–loop–helix (bHLH) motif (Fig. 2E). bHLH proteins function primarily as transcription factors with one helix having basic amino acid residues that facilitate DNA binding. Positive electrostatic charges are localized around the tip of the α5 helix in the C-domain (Fig. 2G). The positively charged surfaces on both domains suggests that they may bind negatively charged molecules, although such molecules are unlikely to be nucleic acids because ARMET is localized in the ER lumen or partly secreted out of cells [7,8].

3.2. Solution dynamics of the ARMET structure

To characterize the dynamic behavior of ARMET in solution, ^{15}N spin-relaxation parameters were measured for backbone amides. Residues within each domain have similar ^{15}N spin-lattice relaxation time (T_1) values (Fig. 3A), but the average T_1 value (0.97 s) for N-domain residues is higher than C-domain residues (0.72 s). Similarities between spin–spin relaxation time (T_2) values of residues within each domain were also found (Fig. 3B), with a slightly greater average T_2 value for the C-domain (77 ms) compared to the N-domain (53 ms). The average T_1/T_2 ratio (19.4, NOE > 0.6) for N-domain residues and that for C-domain residues (9.5, NOE > 0.6) are in largely agreement with the values reported for other globular proteins of comparable size (Fig. S3). These results suggest that both domains are connected by a flexible linker and tumble independently.

To confirm these structural dynamics of the ARMET structure, trypsin digestion of ARMET was performed. The major two fragments (10 and 4 kDa) were produced by the digestion (Fig. 3D). The N-terminal sequence of the lower molecular weight fragment was 113-QIDLS-117 and that of the higher molecular weight fragment was consistent with the N-terminal sequence of the ARMET protein. These results indicate that trypsin cleaved the ARMET protein at the peptide bond between Lys112 and Gln113. These residues are located in the linker region joining the N- and C-domains (Figs. 2H and 3E). These results are consistent with the ^{15}N spin-relaxation results in suggesting that each domain of ARMET moves independently. The positive charge regions on the N- and C-domains may be involved in ligand binding and upon ligand binding the dynamic motion of the two domains may be lost.

In conclusion, we found that the mouse ARMET structure has two domains with positively charged surfaces and each domain fluctuates independently. ARMET may interact with negatively charged molecules such as phospholipids, although this possibility remains to be investigated. Since ARMET is an ER stress-inducible protein required for cell survival [7–10], ARMET may be involved in ER dilation during ER stress and protection of dopaminergic neurons by interacting with phospholipids contained in lipid bilayer membrane. The solution structure of ARMET may facilitate elucidation of the exact function of ARMET in the near future.

Acknowledgements

We thank Y. Kito, K. Senda, and K. Hattori (Nagoya City University) for the preparation of recombinant proteins. This work was supported by Grants-in-Aid for Creative Scientific Research (19GS0314) and Scientific Research (19058008) (to K.N.), The Takeda Foundation (to J.H.), and Grants-in-Aid for Scientific Research on Priority Areas (20059030), Scientific Research on Innovative Areas (20107004), and Scientific Research (21370050) and Nanotechnology Network Project of the Ministry of Education, Culture, Sports, Science and Technology (to K.K.).

Appendix A. Supplementary data

Supplementary data associated with this article can be found, in the online version, at doi:10.1016/j.febslet.2010.03.008.

References

[1] Ellgaard, L. and Helenius, A. (2003) Quality control in the endoplasmic reticulum. Nat. Rev. Mol. Cell Biol. 4, 181–191.
[2] Malhotra, J.D. and Kaufman, R.J. (2007) The endoplasmic reticulum and the unfolded protein response. Semin. Cell Dev. Biol. 18, 716–731.
[3] Bernales, S., Papa, F.R. and Walter, P. (2006) Intracellular signaling by the unfolded protein response. Annu. Rev. Cell Dev. Biol. 22, 487–508.
[4] Yoshioka, M., Kayo, T., Ikeda, T. and Koizumi, A. (1997) A novel locus, Mody4, distal to D7Mit189 on chromosome 7 determines early-onset NIDDM in nonobese C57BL/6 (Akita) mutant mice. Diabetes 46, 887–894.
[5] Ron, D. (2002) Proteotoxicity in the endoplasmic reticulum: lessons from the Akita diabetic mouse. J. Clin. Invest. 109, 443–445.
[6] Yoshinage, T., Nakatome, K., Nozaki, J., Naitoh, M., Hoseki, J., Kubota, H., Nagata, K. and Koizumi, A. (2005) Proinsulin lacking the A7–B7 disulfide bond, Ins2Akita, tends to aggregate due to the exposed hydrophobic surface. Biol. Chem. 386, 1077–1085.
[7] Mizobuchi, N., Hoseki, J., Kubota, H., Toyokuni, S., Nozaki, J., Naitoh, M., Koizumi, A. and Nagata, K. (2007) ARMET is a soluble ER protein induced by the misfolded protein response via ERSE-II element. Cell Struct. Funct. 32, 41–50.
[8] Apostolou, A., Shen, Y., Liang, Y., Luo, J. and Fang, S. (2008) Armet, a UPR-upregulated protein, inhibits cell proliferation and ER stress-induced cell death. Exp. Cell Res. 314, 2454–2467.
[9] Petrova, P. et al. (2003) MANF: a new mesencephalic, astrocyte-derived neurotrophic factor with selectivity for dopaminergic neurons. J. Mol. Neurosci. 20, 173–188.
[10] Palgi, M., Lindstrom, R., Peranen, J., Piepponen, T.P., Saarma, M. and Heino, T.I. (2009) Evidence that DmMANF is an invertebrate neurotrophic factor supporting dopaminergic neurons. Proc. Natl. Acad. Sci. USA 106, 2429–2434.
[11] Kurimoto, T., Asakura, K., Yamasaki, C. and Nemoto, N. (2005) MUSASHI: NMR pulse width determination method by nonlinear least square curve fitting. Chem. Let. 34, 540–541.

[12] Delaglio, F., Vuister, G.W., Zhu, G., Pfeifer, J. and Bax, A. (1995) NMRPipe: a multidimensional spectral processing system based on UNIX pipes. J. Biomol. NMR 6, 277–293.
[13] Guntert, P., Braun, W. and Wuthrich, K. (1991) Efficient computation of three-dimensional protein structures in solution from nuclear magnetic resonance data using the program DIANA and the supporting programs CALIBA, HABAS and GLOMSA. J. Mol. Biol. 217, 517–530.
[14] Cornilescu, G., Delaglio, F. and Bax, A. (1999) Protein backbone angle restraints from searching a database for chemical shift and sequence homology. J. Biomol. NMR 13, 289–302.
[15] Güntert, P., Mumenthaler, C. and Wüthrich, K. (1997) Torsion angle dynamics for NMR structure calculation with the new program DYANA. J. Mol. Biol. 273, 283–298.
[16] Weaver, T.M. (2000) The pi-helix translates structure into function. Protein Sci. 9, 201–206.
[17] Parkash, V., Lindholm, P., Peranen, J., Kalkkinen, N., Oksanen, E., Saarma, M., Leppanen, V.M. and Goldman, A. (2009) The structure of the conserved neurotrophic factors MANF and CDNF explains why they are bifunctional. Protein Eng. Des. Sel. 22, 233–241.
[18] Lindholm, P. et al. (2007) Novel neurotrophic factor CDNF protects and rescues midbrain dopamine neurons in vivo. Nature 448, 73–77.
[19] Bruhn, H. (2005) A short guided tour through functional and structural features of saposin-like proteins. Biochem. J. 389, 249–257.
[20] Kolter, T. and Sandhoff, K. (2005) Principles of lysosomal membrane digestion: stimulation of sphingolipid degradation by sphingolipid activator proteins and anionic lysosomal lipids. Annu. Rev. Cell Dev. Biol. 21, 81–103.
[21] Ahn, V.E., Leyko, P., Alattia, J.R., Chen, L. and Prive, G.G. (2006) Crystal structures of saposins A and C. Protein Sci. 15, 1849–1857.
[22] Koradi, R., Billeter, M. and Wuthrich, K. (1996) MOLMOL: a program for display and analysis of macromolecular structures. J. Mol. Graph. 14, 51–55.